OPEN ACCESS
CellPress

Cell Reports
Article

Conversion of the Thymus into a Bipotent Lymphoid Organ by Replacement of *Foxn1* with Its Paralog, *Foxn4*

Jeremy B. Swann,[1] Annelies Weyn,[1] Daisuke Nagakubo,[1,4] Conrad C. Bleul,[1,5] Atsushi Toyoda,[2] Christiane Happe,[1] Nikolai Netuschil,[1] Isabell Hess,[1] Annette Haas-Assenbaum,[1] Yoshihito Taniguchi,[3,6] Michael Schorpp,[1] and Thomas Boehm[1,*]

[1]Department of Developmental Immunology, Max Planck Institute of Immunobiology and Epigenetics, Stuebeweg 51, 79108 Freiburg, Germany

[2]Comparative Genomics Laboratory, Center for Genetic Resource Information, National Institute of Genetics, Mishima, Shizuoka 411-8540, Japan

[3]Department of Radiation Genetics, Graduate School of Medicine, Kyoto University, Yoshida Konoe, Sakyo-ku, Kyoto 606-8501, Japan

[4]Present address: Division of Biology, Department of Fundamental Biosciences, Shiga University of Medical Science, Seta-Tsukinowa-cho, Otsu, Shiga 520-2192, Japan

[5]Present address: Novartis Institutes for Biomedical Research, Novartis Campus, 4002 Basel, Switzerland

[6]Present address: Department of Preventive Medicine and Public Health, Kyorin University School of Medicine, 6-20-2 Shinkawa, Mitaka, Tokyo 181-8611, Japan

*Correspondence: boehm@immunbio.mpg.de

http://dx.doi.org/10.1016/j.celrep.2014.07.017

SUMMARY

The thymus is a lymphoid organ unique to vertebrates, and it provides a unique microenvironment that facilitates the differentiation of immature hematopoietic precursors into mature T cells. We subjected the evolutionary trajectory of the thymic microenvironment to experimental analysis. A hypothetical primordial form of the thymus was established in mice by replacing FOXN1, the vertebrate-specific master regulator of thymic epithelial cell function, with its metazoan ancestor, FOXN4, thereby resetting the regulatory and coding changes that have occurred since the divergence of these two paralogs. FOXN4 exhibited substantial thymopoietic activity. Unexpectedly, histological changes and a functional imbalance between the lymphopoietic cytokine IL7 and the T cell specification factor DLL4 within the reconstructed thymus resulted in coincident but spatially segregated T and B cell development. Our results identify an evolutionary mechanism underlying the conversion of a general lymphopoietic organ to a site of exclusive T cell generation.

INTRODUCTION

The thymus is a primary lymphoid organ (Miller, 1961) and the site of conventional T cell development in all extant vertebrates (Bajoghli et al., 2011; Boehm, 2011). The formation of a thymopoietic environment and the differentiation of T cells themselves are highly dynamic processes, characterized by complex interactions of different cells types, such as mobile hematopoietic progenitors and resident stromal cells (Anderson and Jenkinson, 2001). Lymphocytes are an ancient component of vertebrate immune systems (Hirano et al., 2013). Differentiation of the different lymphocyte lineages from immature hematopoietic precursors essentially depends on external cues that are provided by lymphopoietic environments. For instance, interleukin-7 (IL-7) and the FLT3 ligand are essential components of the niche supporting the development of B cells (Sitnicka et al., 2003). With respect to T cell differentiation, the required microenvironment is provided by the thymus (Petrie and Zúñiga-Pflücker, 2007). The thymic stroma, which primarily consists of epithelial cells (Rodewald, 2008), generates chemokine gradients that attract lymphoid progenitors (Calderón and Boehm, 2011), provides the Notch ligand DLL4 to initiate specification to the T cell lineage (Hozumi et al., 2008; Koch et al., 2008), orchestrates the selection of self-tolerant antigen receptors clonally expressed on differentiating thymocytes via the provision of self-peptide/major histocompatibility complexes (Kyewski and Derbinski, 2004), and provides the relevant cues supporting the exit of mature T cells into the blood circulation (Zachariah and Cyster, 2010). The thymopoietic process has self-organizing properties; in the presence of a normal hematopoietic system, which generates the necessary lymphoid progenitors, differentiation of thymic epithelial progenitor cells leads to the formation of thymopoietic tissue that supports the generation of a functionally competent T cell repertoire (Bleul et al., 2006).

The differentiation of thymic epithelial progenitors into the various types of mature and functionally distinct thymic epithelial cells (TECs) and the generation of functionally relevant cues supporting T cell development strictly depend on a single transcription factor, FOXN1 (Frank et al., 1999; Nehls et al., 1994). The gene encoding the FOXN1 transcription factor likely emerged in the ancestor common to all vertebrates as a result of the duplication of the *Foxn4* gene, an ancient metazoan gene (Bajoghli et al., 2009). A notable feature of FOXN1 and FOXN4 proteins is nearly identical yet distinct DNA binding

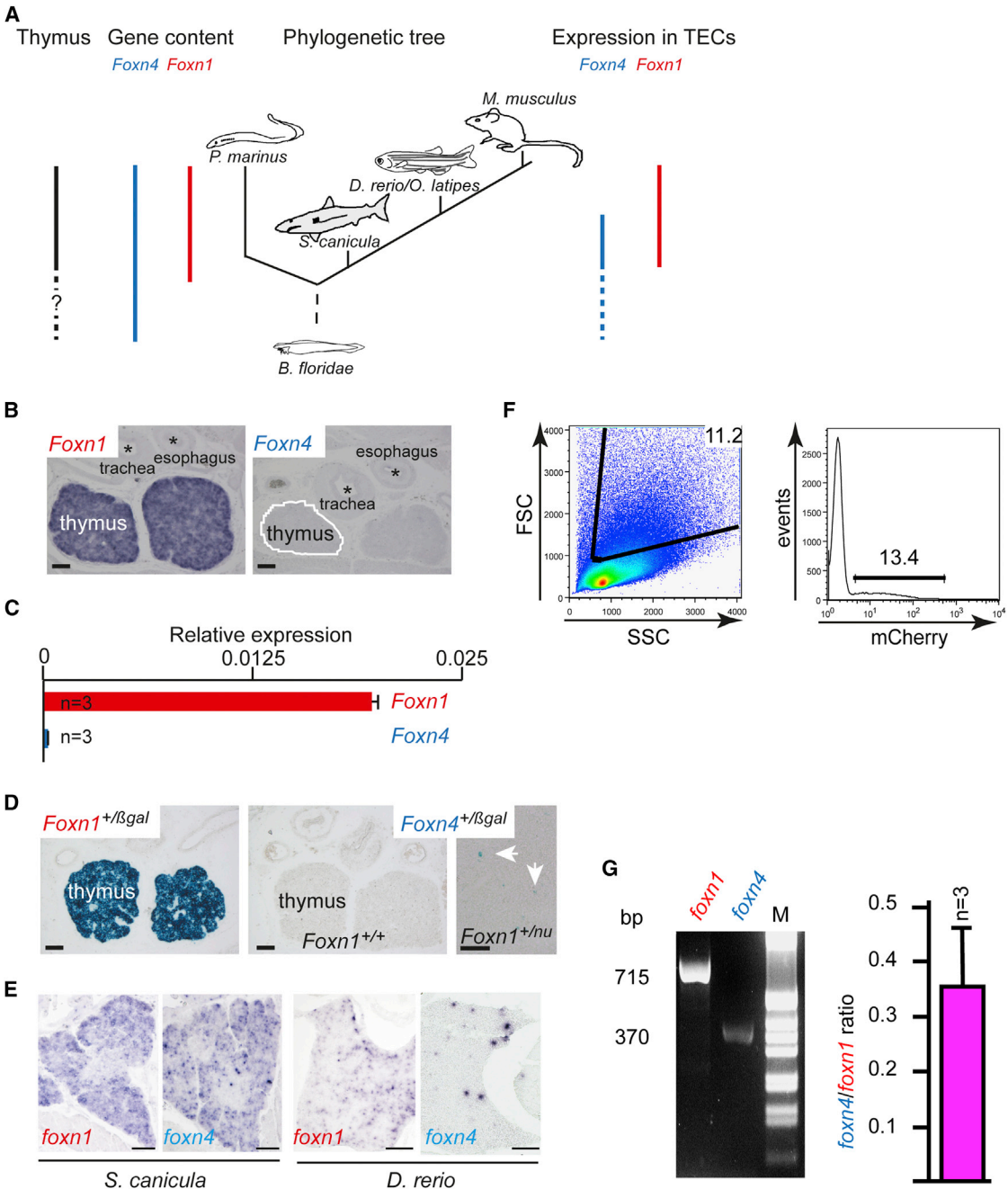

Figure 1. Evolutionary Features of *Foxn4* and *Foxn1* Genes in Vertebrates

(A) Summary of relevant features aligned with a schematic of the chordate phylogenetic tree. The thymus is present in all vertebrates but absent in nonvertebrate chordates. The *Foxn1* gene first appears in vertebrates as a paralog of the ancient *Foxn4* gene. The expression of *Foxn4* in pharyngeal endoderm precedes that of *Foxn1*.

(B) Expression of *Foxn1* and *Foxn4* in E15.5 mouse thymi as determined by RNA in situ hybridization; scale bar, 100 μm.

(C) Quantitative RT-PCR for *Foxn1* and *Foxn4* expression in purified adult mouse TECs relative to β-actin.

(D) X-gal staining of E15.5 mouse thymi from *Foxn1*$^{+/lacZ}$ and *Foxn4*$^{+/lacZ}$ knockin embryos; note that *Foxn4* is expressed at low levels in a small proportion of TECs throughout the thymus, whereas the corresponding analysis of *Foxn1* demonstrated the anticipated ubiquitous expression. Note that *Foxn1*^{nu} represents the original nude allele (Nehls et al., 1994), whereas *Foxn1*^{lacZ} represents a deleterious knockin allele (Nehls et al., 1996). The *nu* allele of *Foxn1* was used here to avoid interference with the detection of β-galactosidase activity derived from the *Foxn4* knockin allele. Scale bar, 100 μm.

(E) *foxn1* and *foxn4* RNA expression in the thymus of *S. canicula* and of *D. rerio* as determined by RNA in situ hybridization. Scale bars, 100 μm.

(F) Light-scatter profile of dissociated thymic cell populations from adult *foxn1:mCherry* transgenic zebrafish. Number indicates percentage of live cells in gate (left). Red fluorescence of gated cells (right); the percentage of positive cells is indicated.

(legend continued on next page)

domains; all vertebrates exhibit the signature residues distinguishing FOXN4 from FOXN1 (Bajoghli et al., 2009). Interestingly, in embryos of the chordate *B. floridae*, which does not possess *Foxn1*, the *Foxn4* gene is expressed in the pharyngeal endoderm, the origin of TECs in all vertebrates (Bajoghli et al., 2009), indicating that the pharyngeal endoderm is an evolutionarily conserved site of expression common to *Foxn4* and *Foxn1* genes. The evolutionary history of the *Foxn4*/*Foxn1* gene family suggests the possibility that, before the emergence of extant vertebrates, thymopoietic function in the pharyngeal endoderm was determined by *Foxn4* rather than *Foxn1*. Thus, we set out to test the idea that *Foxn4* originally possessed thymopoietic activity, that this function was lost during vertebrate evolution as a result of *cis*-regulatory changes, and that its function was taken over by its paralog, *Foxn1*. Exploiting the uniquely favorable features of thymopoiesis, we aimed at examining, in two extant species, zebrafish and mouse, the hypothetical primordial situation of *Foxn4*-driven thymopoiesis focusing on the hematopoietic properties of the resulting organ. Our results are compatible with the hypothesis that the thymus originated as a bipotent lymphopoietic organ, supporting both B and T cell development, and that during the course of vertebrate evolution, it became specialized in orchestrating T cell development at the expense of B cell development.

RESULTS

Expression Patterns of the *Foxn1/4* Gene Family in Vertebrates

The transcription factor FOXN1 (Nehls et al., 1994, 1996) is expressed by TECs, the major constituents of the thymic stroma. It regulates the expression of key target genes such as those encoding the chemokine CXCL12, which is capable of attracting hematopoietic cells to the thymus (Calderón and Boehm, 2012), and the NOTCH1 (Wilson et al., 2001) ligand DLL4, which directs T cell development (Hozumi et al., 2008; Koch et al., 2008; Calderón and Boehm, 2012) in undifferentiated lymphoid progenitors. The essential role of FOXN1 in supporting thymopoiesis is illustrated by the failure of T cell differentiation in mammals lacking a functional *Foxn1* gene (Frank et al., 1999; Nehls et al., 1994). The *Foxn1* gene arose by gene duplication from *Foxn4*, an evolutionarily ancient metazoan gene (Bajoghli et al., 2009). Because both jawless fishes and jawed vertebrates possess *Foxn1* and *Foxn4* genes (Bajoghli et al., 2009), this duplication probably occurred in the extinct ancestor of all vertebrates (Figure 1A). Since paralogous genes are often expressed in partially overlapping domains (Wilkins, 1997), we determined the expression patterns of *Foxn1* and *Foxn4* in the thymus of different vertebrate species. In contrast to *Foxn1*, expression of *Foxn4* cannot be detected by RNA in situ hybridization in the mouse thymus (Figure 1B); this is similar to the situation in the lamprey thymoid (Bajoghli et al., 2011), where only *FOXN1* is expressed. However, more sensitive methods, such as quantitative PCR using RNA extracted from purified mouse TECs (Figure 1C) and X-gal staining of thymic tissue of mice carrying a *Foxn4*^{LacZ} knockin allele (Figure 1D; Figure S1), demonstrated the presence of very low levels of *Foxn4* expression in a small subset of cells in the mouse thymus. Because purification of epithelial cells from the thymoid is not possible at present, an analogous experiment could not be done with the lamprey. Collectively, these results indicate that the thymic microenvironment of living representatives of jawless vertebrates and of mammals is characterized by high levels of *Foxn1* but very low, if any, *Foxn4* expression. Because *Foxn4* is expressed in the pharyngeal endoderm (Bajoghli et al., 2009) of amphioxus, *Foxn4* expression in the thymus might have been lost during the course of vertebrate evolution. If so, coexpression of *Foxn1* and *Foxn4* might still occur in species positioned at intermediate stages of the evolution of vertebrates. This hypothesis is best examined in the jawed vertebrate lineage, where a clear evolutionary sequence is evident. To this end, we examined the expression of *Foxn1* and *Foxn4* genes in the thymus of the cartilaginous fish *S. canicula* (catshark) and the teleosts *D. rerio* (zebrafish) and *O. latipes* (medaka). Expression of both *Foxn1* and *Foxn4* could be demonstrated in the thymi of catshark (Figure 1E), zebrafish (Figure 1E) (Danilova et al., 2004), and medaka (Figure S2A) by RNA in situ hybridization. In order to confirm coexpression of these two genes in TECs, we made use of *foxn1:mCherry* transgenic zebrafish in which TECs express a red fluorescent protein (Figure 1F) (Hess and Boehm, 2012); expression of *foxn4* was clearly demonstrable in *foxn1*-expressing TECs purified by cell sorting (Figure 1G).

Functional Relevance of *Foxn4* Expression in Thymic Epithelial Cells

Considering the contrasting expression patterns of *Foxn1* and *Foxn4* genes in TECs of different vertebrates, we next examined their relative functional significance for thymopoiesis. In the mammalian thymus, *Foxn1* deficiency effectively abolishes any thymopoietic activity in the thymus (Nehls et al., 1994). By contrast, thymopoiesis was unimpaired in *Foxn4*-deficient mice (Figures 2A–2C), compatible with the minimal levels of expression of *Foxn4* in TECs. Other organs, such as the CNS, are however severely affected in the *Foxn4* knockout mice, indicating that we have generated a loss-of-function allele (Figure S1) (Li et al., 2004). Hence, these results indicate that endogenous *Foxn4* expression cannot compensate for the absence of *Foxn1* in the mouse thymus. Next, we examined whether a similar situation exists in fish, where the expression levels of *Foxn1* and *Foxn4* in the thymus are of similar magnitude. To this end, we established a teleost model of *foxn1* deficiency in medaka. Owing to early embryonic lethality as a consequence of heart malformation (Chi et al., 2008), it is not possible to directly examine the impact of *foxn4* deficiency on thymopoiesis in fish. However, two loss-of-function alleles of *foxn1* were identified in medaka (Figure 2D; Figures S2B–2E). Of note, homozygous mutant fish were fertile and survived into adulthood.

(G) Presence of *foxn1* and *foxn4* transcripts (size of cDNA fragments given) in red fluorescent cells from (F) (left). Ratio of *foxn4* and *foxn1* expression in zebrafish TECs as determined by quantitative RT-PCR (right).

In this and all subsequent figures, graphs indicate mean ± SEM, with statistical significance shown (t test) were applicable. See also Figure S1 and Tables S1–S3.

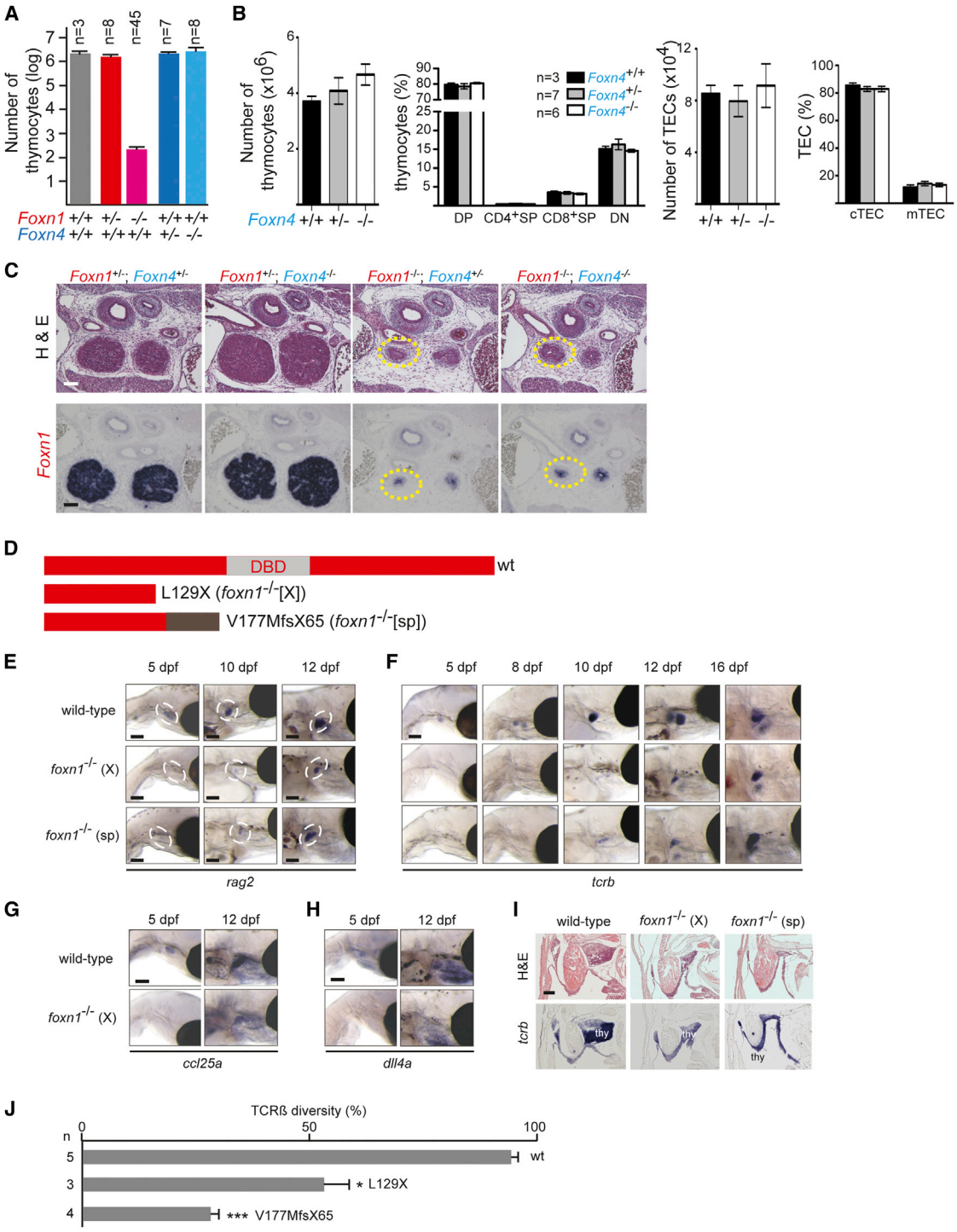

Figure 2. Thymopoietic Function of *Foxn4*

(A) Thymocyte numbers per thymus in *Foxn1*- and *Foxn4*-deficient embryonic day 18.5 mouse embryos. These mice carry loss-of-function *LacZ* knockin alleles.

(B) Normal thymopoiesis in 4-week-old *Foxn4*-deficient mice.

(C) The thymic rudiment is present in $Foxn1^{-/-}$;$Foxn4^{-/-}$ double-deficient mice, as revealed by RNA in situ hybridization with a *Foxn1*-specific probe. The thymic anlage is outlined in yellow. Note that the chimeric *Foxn1* transcript in the $Foxn1^{LacZ}$ knockin allele can be detected by the probe used. Scale bars, 100 μm.

(D) Schematic structure of FOXN1 wild-type and mutant proteins in medaka. In the wild-type protein, the location of the DNA binding domain (DBD) is indicated; the frameshift mutation causes the addition of unrelated protein sequences (gray).

(legend continued on next page)

Detailed analysis of intrathymic T cell development revealed that, while *foxn1* mutants lacked the early phase of thymopoiesis, T cell development resumed at about 8 days postfertilization, as revealed by the expression of *rag2* (Figure 2E) and *tcrb* (Figure 2F). Accordingly, in the thymi of mutant larvae, the expression of known target genes of FOXN1, such as *ccl25a* and *dll4a* (Bajoghli et al., 2009), was initially absent but subsequently became detectable, albeit in a smaller expression domain (Figures 2G and 2H). Thymopoietic activity was maintained in adult mutant fish (Figure 2I); accordingly, *foxn1*-deficient medaka possess a diverse repertoire of T cell receptors (TCRs) in the peripheral T cell compartment, with somewhat lesser diversity than their wild-type siblings (Figure 2J), compatible with their smaller thymus (Figure 2I).

Interestingly, the proteins encoded by *Foxn4* genes of jawed vertebrates exhibit remarkable evolutionary conservation (Figure S3A) (Bajoghli et al., 2009), suggesting that *cis*-regulatory changes rather than modifications of the protein coding regions of *Foxn4* genes underlie the differential contribution to thymopoiesis in vertebrates. Collectively, these results indicate that, unlike the situation in mice, the *foxn1*$^{-/-}$ epithelium of teleost fish possesses the capacity for thymopoiesis. Given the evolutionary relationship between *Foxn4* and *Foxn1* genes (Figure 1A) and the functional importance of *Foxn4* for thymopoiesis in fish (Figure 2), *Foxn4* appears to be a primary candidate for the regulation of tissue-specific functions in the primordial thymic epithelial microenvironment of extinct chordates and/or primitive vertebrates prior to the gene duplication event that gave rise to *Foxn1*.

T Cell Development in *Foxn4*-Expressing Thymic Epithelia

To model the hypothetical primordial situation of *Foxn4*-driven thymopoiesis in mice, we replaced *Foxn1* by *Foxn4* in the mouse thymic epithelium (Figure 3A). To this end, *Foxn1*-deficient mice were supplied with transgenes in which either *Foxn1* (as a control) or *Foxn4* cDNAs were expressed in TECs, under the regulatory elements of the *Foxn1* gene (Bleul and Boehm, 2005) (Figure S3B). Under these conditions, *Foxn4* becomes expressed both in the thymic epithelium (Figures 3B and 3C) and in the hair follicle (Figure S3C), an additional site of *Foxn1* expression in the mouse (Meier et al., 1999). Restoration of normal hair growth not only in *Foxn1*$^{-/-}$;*Foxn1:Foxn1* controls but also in *Foxn1*$^{-/-}$*Foxn1:Foxn4* transgenic mice (Figure S3C) indicates that *Foxn1* promoter elements are capable of regulating transgene expression in a physiologically normal manner and that the expression levels of *Foxn4* are sufficient to achieve coordinate regulation of keratinocyte differentiation in the skin. This observation further supports the notion that the FOXN4 transcription factor activates most, if not all, FOXN1-dependent target genes, which is compatible with their similar DNA binding specificities (Nakagawa et al., 2013; Schlake et al., 1997). With respect to the thymus, we found a normal histological structure in control *Foxn1*$^{-/-}$;*Foxn1:Foxn1* transgenic mice (Figure 3D) and a normal pattern of T cell development (Figure 3E). Surprisingly, *Foxn4* expression also restored failing thymopoiesis in *Foxn1*$^{-/-}$ mice. In *Foxn1*$^{-/-}$;*Foxn1:Foxn4* transgenic mice, the thymus is characterized by regions of varying cellular density, reminiscent of cortical and medullary areas in the wild-type thymus, although some cystic regions persist (Figure 3D). Despite these histological perturbations, the major thymocyte populations were present (Figure 3E). In *Foxn1*$^{-/-}$;*Foxn1:Foxn4* transgenic mice, the absolute number of thymocytes attained up to 30% of normal levels, albeit with considerable variation among individual mice (Figure 4A); one notable difference to wild-type or *Foxn1*$^{-/-}$;*Foxn1:Foxn1* transgenic mice is the considerable increase in the proportion of CD4^{-}/CD8^{-} cells (Figure S4A), which will be addressed in more detail below. The thymopoietic activity in reconstituted transgenic mice led to the presence of large numbers of peripheral T cells in the spleen (Figure 4B) and lymph nodes (Figure 4C), reaching almost normal levels in *Foxn1*$^{-/-}$;*Foxn1:Foxn1* transgenic mice and subnormal levels in *Foxn1*$^{-/-}$;*Foxn1:Foxn4* mice (Figures 4B and 4C), with some indication of oligoclonality of the T cell repertoire in the latter group (Figure 4D; Figure S4B). As judged by several criteria, the peripheral T cell compartments in transgenic mice appear to be functionally competent. For instance, T cells isolated from the lymph nodes of reconstituted mice proliferated in response to TCR crosslinking in vitro (Figure 4E). In accordance with the restoration of thymopoiesis, the majority of *Foxn1*$^{-/-}$;*Foxn1:Foxn4* mice mounted hapten antibody responses (Figure 4F), in line with the varying extent of thymopoietic activity (Figures 4A–4D). *Foxn1*$^{-/-}$;*Foxn1:Foxn4* mice had a normal lifespan and did not exhibit overt autoimmune phenomena, compatible with the presence of FOXP3+ regulatory T cells (Figure 4G). Collectively, these data indicate that T cell immunity was restored in *Foxn1*$^{-/-}$ mice expressing *Foxn4* in the thymic epithelium. Together, these results support the notion that, when expressed at sufficiently high levels in thymic epithelial cells (TECs), FOXN4 can at least partially replace FOXN1 in supporting thymopoietic functions not only in fish but also in mice.

Characteristics of *Foxn4*-Driven Thymic Microenvironment

Next, we carried out a more detailed examination of the structural and functional properties of thymi in *Foxn1*$^{-/-}$;*Foxn1:Foxn4* mice. The overall numbers of TECs in the reconstituted thymi are comparable (Figure 5A). Cortical (cTECs; CD45^{-}EpCam^{+} Ly51^{+}UEA1^{-}) and medullary (mTECs; CD45^{-}EpCam^{+}Ly51^{-} UEA1^{+}) lineages of TECs, which together determine the thymopoietic capacity of the thymic microenvironment, are both present, as determined by their cell-surface phenotype, in *Foxn1*$^{-/-}$;*Foxn1:Foxn4* mice (Figure 5B), although cTECs predominate (Figure 5C). While fewer in number, mTECs in

(E–H) Thymopoiesis in *foxn1*-deficient medaka; whole-mount RNA in situ hybridization for *rag2* (E), *tcrb* (F), *ccl25a* (G), and *dll4a* (H) for wild-type fish and mutants at various time points; dpf, days after fertilization. Scale bars, 100 μm.

(I) Histological appearance of fish thymi at 6 weeks of age. Hematoxylin/eosin staining (upper panels), and *tcrb* RNA in situ hybridization (lower panels).

(J) Diversity of peripheral Vß5-Cß2 TCR sequences; *p < 0.05; ***p < 0.001. Scale bars, 100 μm.

See also Figure S2 and Tables S1–S3.

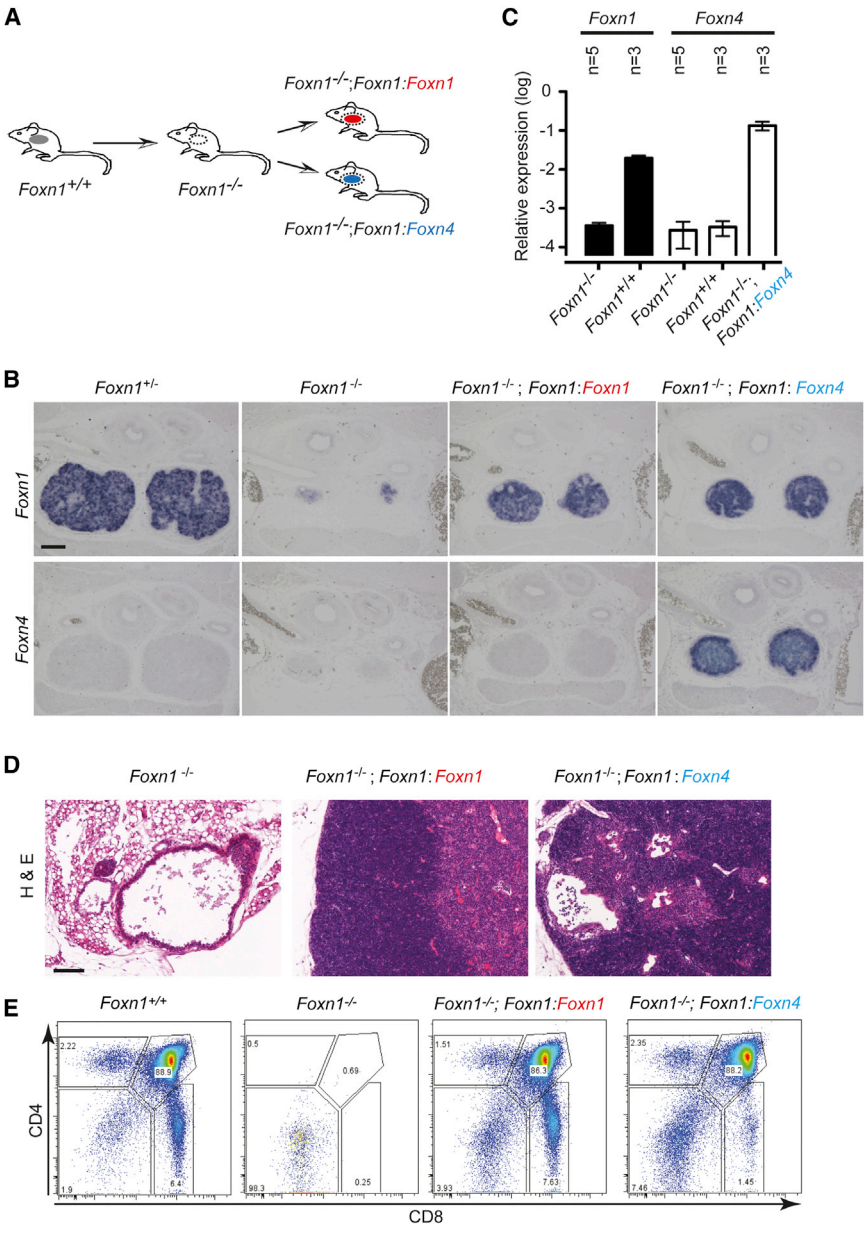

Figure 3. *Foxn4*-Driven Thymopoiesis in Mice

(A) Schematic of transgenic expression of *Foxn1* or *Foxn4* in TECs of *Foxn1*-deficient mice. In the absence of FOXN1 function, TECs do not differentiate (dotted line); transgenic expression of *Foxn1* (red oval) or *Foxn4* (blue oval) in the *Foxn1*-deficient background restores thymopoiesis.

(B) Expression of transgenes as revealed by RNA in situ hybridization with *Foxn1*- and *Foxn4*-specific probes. Note the small thymic rudiment in nontransgenic $Foxn1^{-/-}$ mice that becomes considerably larger in the transgenic animals; *Foxn4* expression is detectable only in the *Foxn4* transgenic mice. Scale bar, 100 μm.

(C) Expression of *Foxn1* and *Foxn4* relative to *β-actin* in purified TECs of adult mice as detected by quantitative RT-PCR. The primers used for quantitative PCR also detect the mutant *Foxn1* transcript.

(D) Histological sections of thymic rudiments/thymi of adult mice (hematoxylin and eosin staining). Scale bar 100 μm.

(E) Flow cytometric profiles of thymocytes of adult mice stained with antibodies directed against the coreceptors CD4 and CD8.

See also Figure S3 and Tables S1–S3.

$Foxn1^{-/-}$;*Foxn1:Foxn4* mice appear to execute a normal differentiation program, as revealed by expression of CD80 (Figure 5D), major histocompatibility complex (MHC) class II (Figure 5E), and *Aire* (Figure 5F), the regulator of tissue-restricted antigen expression associated with central tolerance induction (Mathis and Benoist, 2009); these observations are compatible with the absence of autoimmunity in the reconstituted mice. Interestingly, despite the seemingly normal patterns of differentiation of TECs in the thymi of $Foxn1^{-/-}$;*Foxn1:Foxn4* mice, the expression of cytokeratins appears to be abnormal. Unlike in the wild-type situation, where cortical and medullary areas are well separated, the majority of $Foxn1^{-/-}$;*Foxn1:Foxn4* TECs co-express the cortical marker keratin 8 and the medullary marker keratin 5 (Figure 5G). However, as indicated by their cell-surface phenotypes, these TECs are not immature (as is presumed to be the case for K5/K8 double-positive TECs in the wild-type thymus; Rodewald, 2008) but instead represent an unusual yet functionally competent state of differentiation.

Characteristics of *Foxn4*-Driven Hematopoietic Properties

With respect to the hematopoietic compartment, the thymi of $Foxn1^{-/-}$;*Foxn1:Foxn4* transgenic mice contained cells at all stages of T cell differentiation (Figures 3 and 4). However, the proportion of $CD4^{-}/CD8^{-}$ double-negative thymocytes is significantly increased (Figures 4A and 6A), owing to a sizeable population of B cells (Figure 6B). In contrast to the wild-type situation, the thymi of $Foxn1^{-/-}$;*Foxn1:Foxn4* mice contained large numbers of proliferating immature B cells (Figures 6C and 6D), resembling the situation in the bone marrow (Hardy and Hayakawa, 2001) (Figures S5A–S5C) and indicating the presence of intrathymic B cell poiesis. It is important to note that the hematopoietic phenotype of the thymi of $Foxn1^{-/-}$;*Foxn1:Foxn4* mice (that is, the coexistence of T and B cell poiesis) has not been previously observed in situations of impaired T cell development (Akashi et al., 2000; Ceredig, 2002; Hozumi et al., 2008; Koch et al., 2008; Wilson et al., 2001); for instance, the fraction of B cells in the thymus of $Foxn1^{-/-}$;*Foxn1:Foxn4* mice is far greater than that observed in T cell-deficient $Cd3e^{-/-}$ mice (Figure S5D) and thus is not the result of a simple reduction of T cells in the thymus.

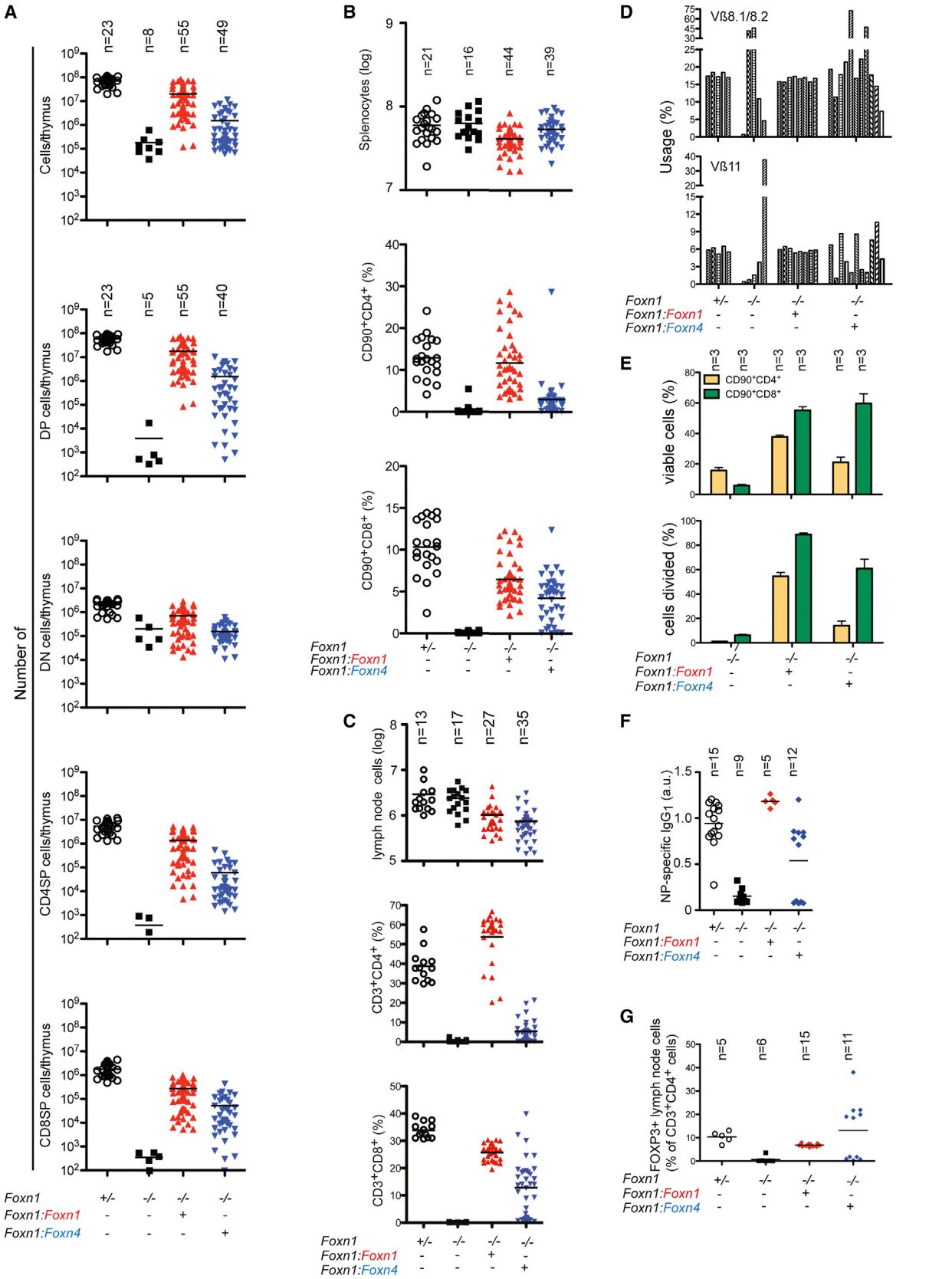

(legend on next page)

Moreover, the preponderance of B cells in the thymus of *Foxn1*$^{-/-}$;*Foxn1:Foxn4* mice is not the sign of premature aging of the thymic environment, as the thymi of old mice do not exhibit this phenotype (Figure S5E). Collectively, these studies indicate that *Foxn4*-expressing epithelia generate a microenvironment that is conducive not only to T cell poiesis but also to B cell poiesis.

Formation of a Fish-like Thymus in Mice

In fish, B cells are readily detectable in the thymus (Vigliano et al., 2011; DeLuca et al., 1983; Miyadai et al., 2004; Sood et al., 2011, 2012) as well as in the kidney (Figure 6E), the major hematopoietic site in teleosts; the proportion of B cells in the fish thymus can reach up to 5%. B cells remain in the fish thymus even in the absence of *foxn1* (Figure S5F), indicating that coexpression of *foxn4* and *foxn1* genes in TECs of the fish thymus supports B cell development alongside T cell development (Figure 2). This observation allowed us to carry out a direct test of the validity of our strategy of modeling evolutionarily ancient thymopoietic environments in mice. If coexpression of *Foxn1* and *Foxn4* in the mouse thymic epithelium indeed generates the equivalent of an ancient form of a thymic microenvironment, it should exhibit fish-like hematopoietic properties. This proved to be the case. When the thymus of *Foxn1*$^{-/-}$;*Foxn1:Foxn1*; *Foxn1:Foxn4* double-transgenic mice was examined, several differences to the single transgenic situations were noted. First, we found that thymic cellularity in the double-transgenic mice was about 10-fold higher than that of *Foxn1*$^{-/-}$;*Foxn1:Foxn4* mice and approached that of *Foxn1*$^{-/-}$;*Foxn1:Foxn1* mice (Figure 6F); this was accompanied by intermediate features with respect to the proportions of CD4^{+}/CD8^{+} double-positive thymocytes (Figure 6G) and CD4^{-}/CD8^{-} thymocytes (Figure 6H). In terms of absolute numbers of B cells, the double-transgenic mice contained about 100-fold more B cells than *Foxn1*$^{-/-}$;*Foxn1:Foxn1* mice and about 5-fold more than *Foxn1*$^{-/-}$;*Foxn1:Foxn4* mice (Figure 6I); a similar picture emerged for the absolute numbers of immature B cells (Figure 6J). This result supports the notion that coexpression of *Foxn4* and *Foxn1* in TECs underlies the phenotypic characteristics of the fish thymus.

Spatial Segregation of T and B Cell Development

Next, we examined the properties of the hypothetical primordial thymus generated by sole expression of *Foxn4* in greater detail. In contrast to T cells, which locate to the epithelial compartment (Figures 6K and 6L), B cells in the thymi of *Foxn1*$^{-/-}$;*Foxn1:Foxn4* mice exhibit an abnormal anatomical distribution. In the wild-type thymus, B cells represent about 0.1% of hematopoietic cells (Akashi et al., 2000; Flores et al., 2001), the majority of which are mature B cells; these are located at the corticomedullary junction, whereas the small fraction of immature B cells are distributed across the entire thymus (Akashi et al., 2000) (Figure 6M). By contrast, in the reconstituted thymi of *Foxn1*$^{-/-}$;*Foxn1:Foxn4* mice, B cells predominantly located to the perivascular space of intrathymic vessels composed of ERTR7-positive mesenchymal cells (Figure 6N).

Mechanistic Basis for B Cell Development in *Foxn4*-Driven Lymphopoiesis in the Thymus

To gain insight into the mechanism by which *Foxn4* expression induces a bipotent lymphopoietic thymic microenvironment, we first focused on FOXN1 target genes in the thymic epithelium. Although related, the DNA binding domains (DBDs) of FOXN4 and FOXN1 are clearly distinct (Figure 7A). Our earlier work demonstrated that four FOXN1-dependent factors (CCL25, CXCL12, KITL, and DLL4) determined the hematopoietic properties of the thymus (Calderón and Boehm, 2012). In TECs isolated from the thymus of *Foxn1*$^{-/-}$;*Foxn1:Foxn4* mice, all four factors are expressed, albeit to different degrees relative to the wild-type situation (Figure S6A). This suggested the possibility of functional divergence of the DBDs of FOXN4 and FOXN1 transcription factors (Figure 7A). To address this issue directly, we established an additional transgenic line, expressing a chimeric transcription factor containing the DBD of FOXN4 in the context of the FOXN1 protein, designated FOXN1/4 (Figure 7B). The fraction of immature B cells in the thymi of *Foxn1*$^{-/-}$;*Foxn1:Foxn1/4* mice was as high as that in *Foxn1*$^{-/-}$;*Foxn1:Foxn4* mice, indicating that the DBD is a major determinant of this aspect of FOXN4 function (Figure 7C). Intriguingly, we observed that, whereas the expression levels of *Dll4* are identical to the wild-type situation in *Foxn1*$^{-/-}$;*Foxn1:Foxn1* mice, the expression levels of *Dll4* in the thymi of *Foxn1*$^{-/-}$;*Foxn1:Foxn4* and *Foxn1*$^{-/-}$;*Foxn1:Foxn1/4* mice are both reduced to a similar extent (Figure 7D). Based on our previous work, which positioned DLL4 at the top of the functional hierarchy of the other three FOXN1-dependent factors (CCL25, CXCL12, and KITL) (Calderón and Boehm, 2012), we hypothesized that an additional factor might play a role in generating the B cell poietic environment in the thymi of *Foxn1*$^{-/-}$;*Foxn1:Foxn4* mice. To this end, we examined the potential role of IL-7, which is a general lymphopoietic factor important for both T and B cell development.

Figure 4. Thymopoiesis in Adult Transgenic Mice

(A) Thymocyte populations are shown. DP, thymocytes expressing both CD4 and CD8; DN, thymocytes expressing neither CD4 nor CD8; CD4SP, thymocytes expressing only CD4; CD8SP, thymocytes expressing only CD8.

(B) Splenocyte populations in adult transgenic mice of the indicated genotypes.

(C) Characterization of lymph node cells in adult transgenic mice of the indicated genotypes. Total cellularity of lymph nodes (top panel) and proportions of lymph node CD4^{+} (middle panel) and CD8^{+} (bottom panel) T cells.

(D) TCR Vß usage in adult transgenic mice of the indicated genotypes as determined by flow cytometry. Each bar represents the percentage of CD4^{+} (left) and CD8^{+} (right) splenic T cells from an individual mouse that utilize the indicated Vß segment.

(E) In vitro stimulation of lymph node cells of the indicated phenotypes with anti-CD3. Viable cells were identified as hydroxystilbamidine negative, and the proportion of divided cells (CD4^{+} or CD8^{+}) was determined by CSFE content.

(F) Anti-NP immunoglobulin G1 titers after immunization of adult mice with CGG-NP in arbitrary units (a.u.).

(G) Fraction of FOXP3^{+} Treg cells among lymph node CD4^{+} T cells.

The numbers of mice analyzed per genotype are indicated. See also Figure S4 and Table S3.

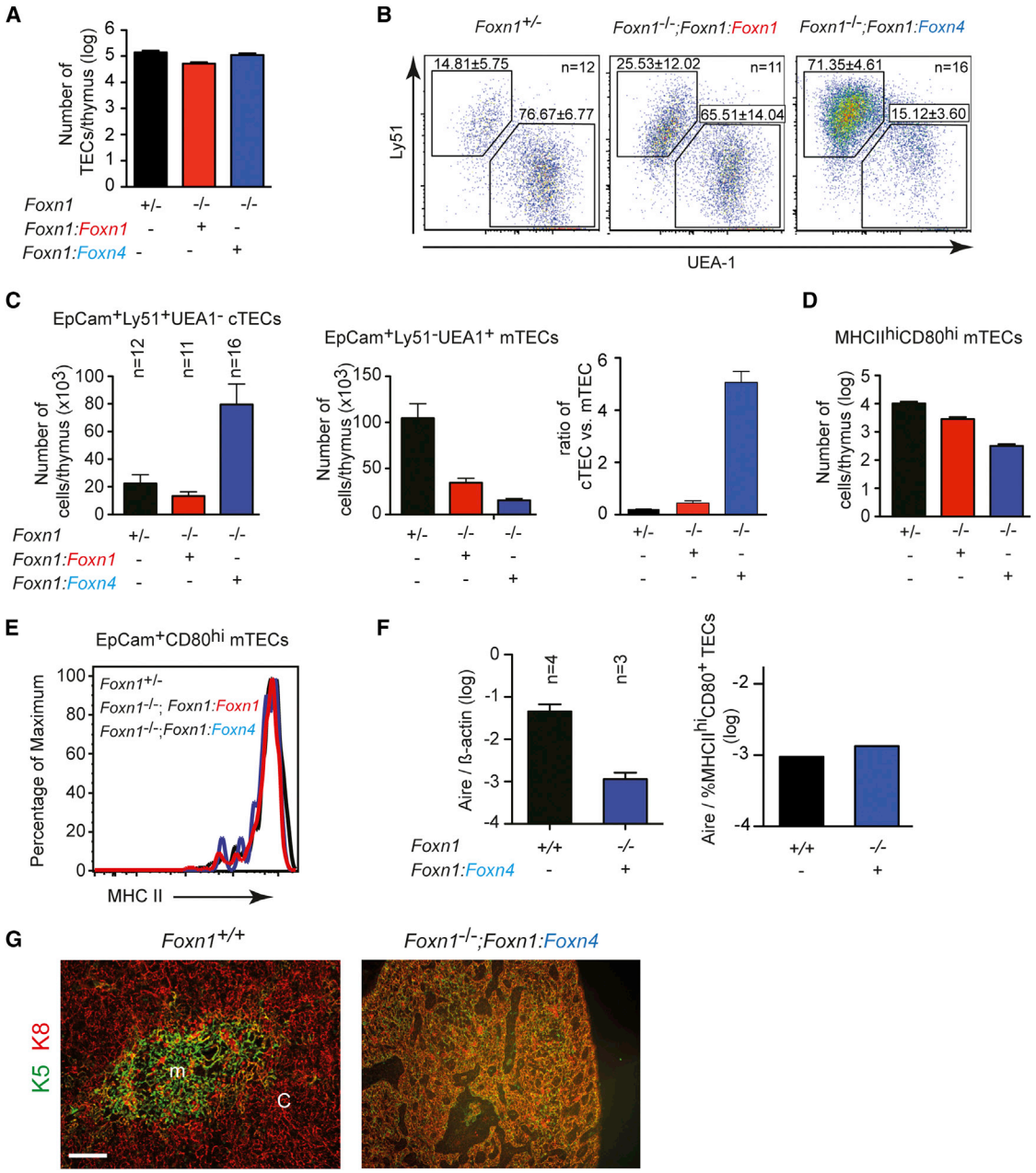

Figure 5. Characterization of the Epithelial Compartment in the Adult Thymus

(A) Absolute numbers of total thymic epithelial cells (TECs).

(B) Distribution of TEC subsets; percentages of total TECs are given above the respective gates.

(C) Absolute numbers of cortical (left) and medullary (middle) TECs; the ratio of cTECs to mTECs is indicated (right panel).

(D) Absolute numbers of mature medullary TECs.

(E) Expression levels of MHC class II on mature mTECs.

(F) Expression of *Aire* relative to β-*actin* in purified total TECs as determined by quantitative RT-PCR; the reduced level in transgenic epithelia corresponds to the absolute reduction of the mature mTEC population (see right panel).

(G) Immunohistochemical detection of keratin expression reveals distinct medullary (m; keratin 5, K5) and cortical (c; keratin 8, K8) regions in wild-type thymi (left); the thymi of *Foxn1*$^{-/-}$;*Foxn1:Foxn4* transgenic mice (right panel) exhibit irregular appearance and frequent coexpression of the two keratins. Scale bar, 100 μm. See also Tables S2 and S3.

Importantly, expression of the *Il7* gene is independent of FOXN1 (Zamisch et al., 2005) (Figure S6B), suggesting the possibility that the reduced expression of *Dll4* might change the hematopoietic properties of the thymic microenvironment. As expected, expression levels of *Il7* in *Foxn1*$^{-/-}$;*Foxn1:Foxn1*, *Foxn1*$^{-/-}$;*Foxn1:Foxn4*, and *Foxn1*$^{-/-}$;*Foxn1:Foxn1/4* mice were found to

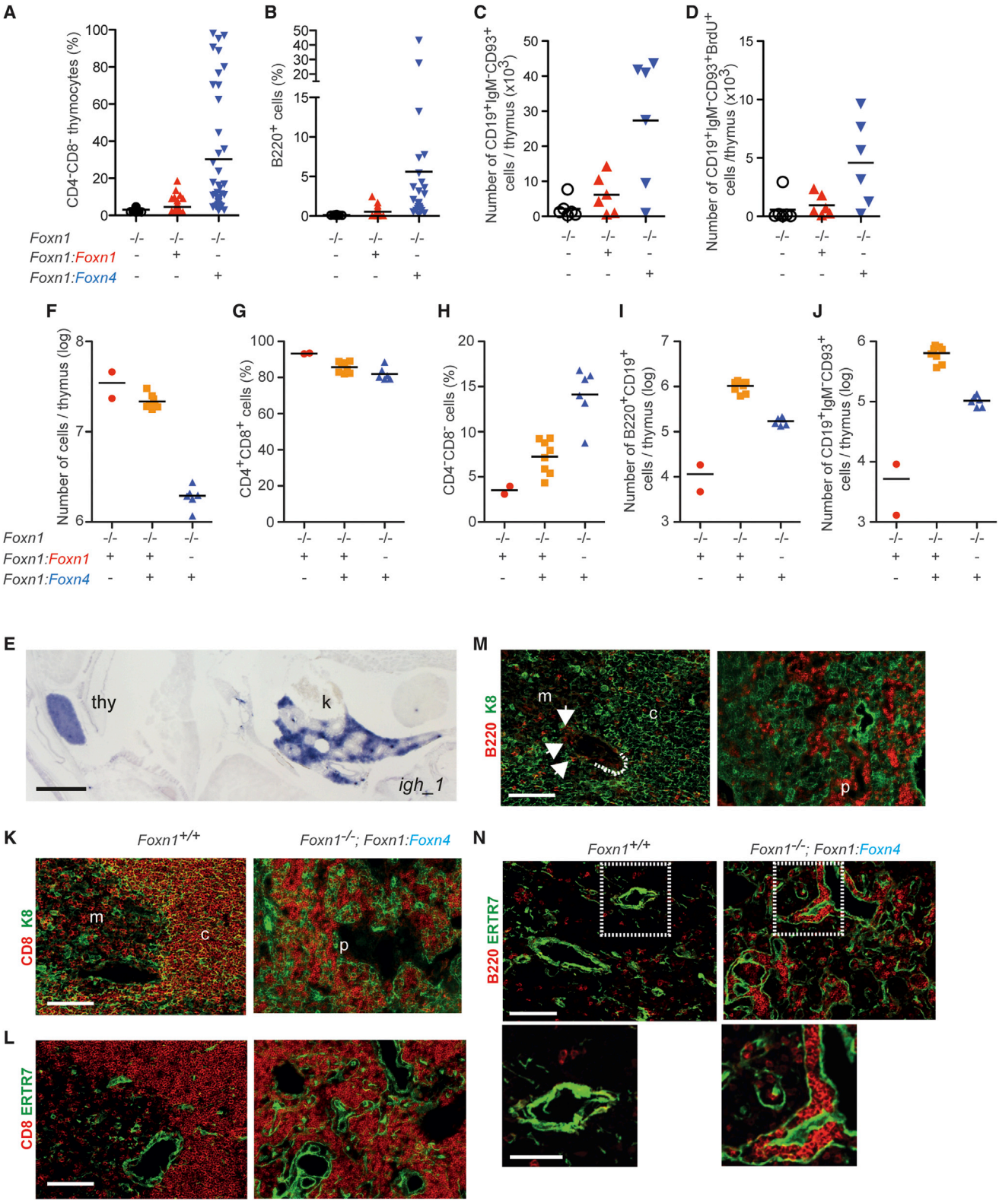

Figure 6. B Cell Poiesis in the Reconstituted Thymi of 4-Week-Old *Foxn1*$^{-/-}$;*Foxn1:Foxn4* Mice

(A) Proportion of CD4^{-}/CD8^{-} double-negative thymocytes.

(B) Proportion of thymocytes with B cell phenotype.

(legend continued on next page)

be similar to those in wild-type mice (Figure S6C). This led to a consistent reduction in the ratio of *Dll4* and *Il7* gene expression by about two-thirds (Figure 7E).

To directly examine the possibility that the disbalance between *Dll4* and *Il7* expression determines the extent of B cell poiesis in the thymus, we generated additional transgenic mice overexpressing these factors in the thymic microenvironment. Indeed, increased *Il7* levels in the microenvironment of the wild-type thymus (equivalent to an overall lower *Dll4*/*Il7* ratio) substantially increased the number of immature B cells; by contrast, overexpression of *Dll4* alone (equivalent to a higher *Dll4*/*Il7* ratio) or coexpression of *Il7*− and *Dll4*− transgenes did not favor B cell poiesis (Figure 7F).

DISCUSSION

Evolutionary novelties are thought to be the result of qualitative changes in the genetic material, such as diverging coding capacities of the genome, changes in regulatory regions of genes, and the reorganization of genetic networks (Peter and Davidson, 2011). While functional changes associated with the evolutionary trajectory of a particular molecular or morphological trait can be easily examined in extant species, comparative studies often suggest that the origin of a particular innovation must have occurred in an extinct species. Hence, functional interrogations of presumed ancestral states of cytological and morphological innovations present significant challenges.

Hematopoietic tissues are ideal targets for phylogenetic studies of complex tissues, due to the fact that their hematopoietic capacity is largely determined by the structure and functionalities of their organotypic microenvironments. For instance, our previous work demonstrated how the thymus, which is the site of T cell development in all vertebrates, can be changed into a tissue supporting the development of mast cells instead of lymphocytes (Calderón and Boehm, 2012).

Another favorable characteristic of the hematopoietic system in this context is the fact that it has deep roots in metazoan evolution (Hartenstein, 2006). With respect to lymphocytes, recent findings suggest that B- and T-like lineages already emerged in the ancestor of all vertebrates, preceding the evolution of molecularly distinct somatically diversifying receptor types (Hirano et al., 2013).

The fact that in vertebrates T cell development always occurs in the thymus (Boehm et al., 2012) represents an additional (methodological) advantage for tissue re-engineering. Whereas the sites of B cell development in vertebrates are highly variable, ranging from derivatives of the gut in basal vertebrates to the bone marrow in mammals (Boehm et al., 2012), the observation that *FOXN4* is expressed in the pharyngeal endoderm of the basal chordate amphioxus (Bajoghli et al., 2009) suggests that this region was preadapted to subsequently develop into a lymphopoietic tissue. Hence, because only a single tissue type must be subjected to experimental manipulation, in vivo modeling of different stages of the evolutionary trajectory of thymopoietic tissues is greatly facilitated.

Evolutionary Trajectory of Thymopoietic Tissues

Our results indicate that the development and function of thymopoietic tissues were initially supported by the expression of the FOXN4 transcription factor. Following a gene duplication event that gave rise to FOXN1, the thymus evolved via an intermediate state of FOXN4 and FOXN1 coexpression into a state of sole FOXN1 expression. An important validation of our experimental strategy was the successful recapitulation in mice of the distinctive hematopoietic properties peculiar to the fish thymus. We established that coexpression of FOXN4 and FOXN1 in TECs generated a thymus geared toward T cell development but with a substantial degree of B cell development. In the hypothetical primordial version of the thymopoietic microenvironment that expresses only FOXN4, this lymphopoietic bipotency was even more pronounced, to such an extent that the thymus harbored almost as many B cells as T cells. Hence, our studies suggest a plausible scenario for the transition of a bipotent lymphopoietic tissue to a lymphoid organ supporting primarily T cell development.

The lymphopoietic properties of the hypothetical primordial thymus suggested an intriguing mechanism regulating the outcome of lymphocyte differentiation in the thymus. Indeed, the phenotypes observed in mice transgenically overexpressing IL-7 or DLL4 in the stromal compartment of the thymus confirmed our hypothesis that the outcome of lymphocyte

(C) Absolute numbers of immature B cells.
(D) Absolute numbers of proliferating immature B cells.
(E) Presence of B cells in the adult fish thymus (*O. latipes*) as detected by RNA in situ hybridization with an immunoglobulin heavy chain-specific probe (*igh_1*); note the comparable signal strengths in kidney (k), the primary site for B cell poiesis in fish, and the thymus (thy).
(F) Absolute numbers of thymocytes.
(G) Proportion of $CD4^+/CD8^+$ DP thymocytes.
(H) Proportion of $CD4^-/CD8^-$ double-negative thymocytes.
(I) Absolute numbers of B cells.
(J) Absolute numbers of immature B cells.
(K) Immunohistochemical detection of intrathymic $CD8^+$ T cells and K8-positive epithelial cells; m, medulla; c, cortex; p, perivascular space. Scale bar, 100 μm.
(L) Immunohistochemical detection of intrathymic $CD8^+$ T cells and $ERTR7^+$ mesenchymal cells. Scale bar, 100 μm.
(M) Immunohistochemical detection of intrathymic $B220^+$ B cells and K8-positive cortical epithelial cells; m, medulla; c, cortex; p, perivascular space (arrows); dashed line, location of corticomedullary junction. Scale bar, 100 μm.
(N) Immunohistochemical detection of intrathymic $B220^+$ B cells and $ERTR7^+$ mesenchymal cells; scale bar, 100 μm. A higher magnification of the indicated region is shown in insets; scale bar, 50 μm.
See also Figure S5 and Table S3.

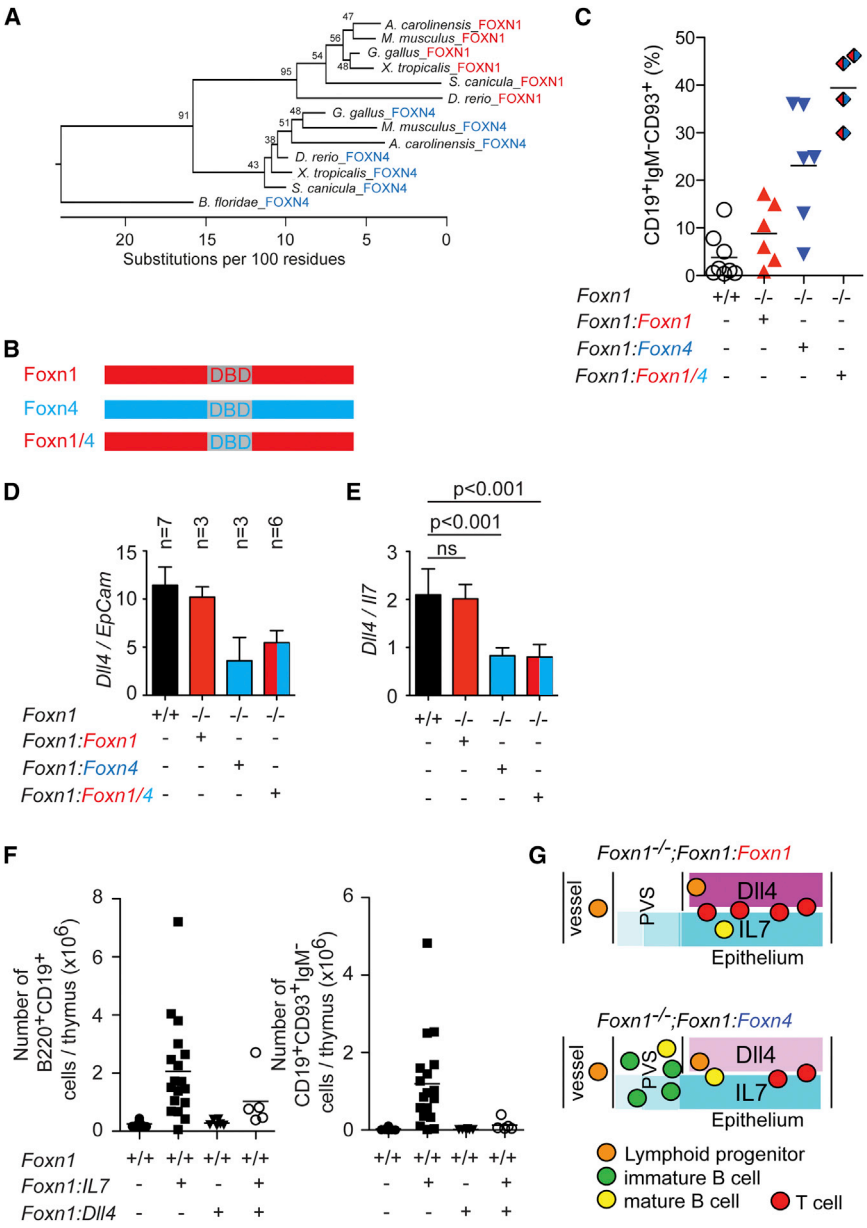

Figure 7. Mechanism Underlying the Bipotent Nature of Lymphopoiesis in the Thymus

(A) Phylogenetic analysis of FOXN1 and FOXN4 based on protein sequences of the DNA binding domain (DBD); some sequences encoding the wing region were shortened to enhance alignment (for source sequences, see Supplemental Experimental Procedures).

(B) Schematic of transcription factors used. Red boxes indicate FOXN1-derived sequences, and blue boxes FOXN4-derived sequences; gray shading indicates the DBD and the color of letters the origin of the sequences.

(C) Proportion of thymic $CD19^+$ B cells with immature phenotype in 4-week-old mice.

(D) Expression levels of *Dll4* relative to *Epcam* in the thymi of 4-week-old *Foxn1*-deficient mice transgenic for the indicated transcription factors.

(E) Expression levels of *Dll4* relative to *Il7* in the thymi of 4-week-old *Foxn1*-deficient mice transgenic for the indicated transcription factors; one-way ANOVA Bonferroni-corrected multiple comparisons.

(F) Absolute numbers of total B cells (left) and immature B cells (right) in thymi of 4-week-old transgenic mice.

(G) Schematic illustrating the presence of B cell poiesis in the perivascular space (PVS) under conditions of reduced DLL4 but unchanged IL-7 expression levels.

See also Figure S6 and Tables S2 and S3.

differentiation in the thymus is achieved through the balance between a general lymphopoietic factor (IL-7) and a lineage specification factor (DLL4). However, it is conceivable that, in addition to distinct lymphopoietic characteristics, the transition of FOXN4 to FOXN1 also affected other features of the thymic microenvironment, such as the emergence of segregated cortical and medullary areas. Nonetheless, the shift toward a T-centric lymphopoietic thymic microenvironment during vertebrate evolution appears to have been primarily achieved by changes in expression levels of *Dll4* in TECs, a key target gene of both FOXN4 and FOXN1. This constitutes a clear and biologically relevant example of the differential function of these two genes that contributes to thymic development and its lymphopoietic properties.

Like many, if not all, transcription factors, FOXN1 and FOXN4 have multiple distinct functions in different tissues, owing to their complex patterns of expression and/or presence of cofactors in certain cell types. For instance, FOXN1 not only regulates the differentiation of TECs (Nehls et al., 1996) but also is required for proper keratinization of the hair shaft (Meier et al., 1999). Similarly, in addition to the thymopoietic function identified here, FOXN4 is, for instance, required for heart development (Chi et al., 2008). These observations illuminate shared and divergent aspects of the evolutionary trajectories of these two paralogous genes.

Anatomical Separation of Developing Lymphoid Lineages in the Hypothetical Primordial Thymus

Homing to the thymus is a dynamic process that is characterized by repeated inward and outward migration of lymphoid progenitor cells (Hess and Boehm, 2012); hence, some of the lymphoid progenitors (the phenotypic characteristics of which are currently unknown; Awong and Zuniga-Pflucker, 2011) migrating into the thymus might not be exposed to sufficiently high levels of membrane-bound DLL4 (relative to the diffusible cytokine IL-7) during their initial encounters with the thymic microenvironment of *Foxn1*$^{-/-}$;*Foxn1:Foxn4* mice to commit them to the T cell

lineage, resulting instead in specification to B cells (Figure 7G). Indeed, it has been previously shown that the FLT3 ligand, a key component of the microenvironment supporting B cell development in the bone marrow (Sitnicka et al., 2003), is expressed by perivascular fibroblasts in the thymus (Kenins et al., 2008). Thus, the perivascular space in the thymus provides an environment suitable for B cell development when the availability of signals promoting T cell specification is suboptimal. The bipotent lymphoid capacity of the thymus in *Foxn1*$^{-/-}$;*Foxn1:Foxn4* mice thus combines the features of the two principal but anatomically segregated primary lymphoid organs in extant mammals: the thymus, whose epithelial environment specializes in supporting T cell differentiation, and the bone marrow, whose mesenchymal environment supports B rather than T cell development.

Although T and B cells develop in distinct microenvironments of the reconstructed primordial thymus, it is unclear whether these T and B cells arise from a common lymphoid progenitor that is recruited to the thymus and subsequently differentiates within specific thymic niches or whether T and B cells derive from distinct, lineage-committed progenitors preprogrammed toward T or B cell fates prior to their recruitment to the thymus. Lineage-tracing studies indicated that B cells are generated in the thymus via both cell-intrinsic (requiring Notch signaling) and cell-extrinsic (not requiring Notch signaling) pathways (Feyerabend et al., 2009). It will be interesting to examine to which extent these two pathways contribute to B cell development in the primordial thymus.

In conclusion, the present analysis of the evolutionary trajectory of the FOXN4 and FOXN1 transcription factors illustrates how *cis*-regulatory (Peter and Davidson, 2011) and protein (Soskine and Tawfik, 2010) changes synergized to facilitate the emergence of functional novelty underlying the cellular arm of adaptive immunity in mammals.

EXPERIMENTAL PROCEDURES

Mice

Foxn1:Foxn1, *Foxn1:Il7*, *Foxn1:Foxn4*, *Foxn1:Foxn1/Foxn4chimaera* and *Foxn4*^{lacZ} knockin transgenic mice were generated and characterized according to standard protocols; all other transgenic mouse lines were described earlier (see the Supplemental Experimental Procedures for details).

Fish

Mutations in the medaka *foxn1* gene were identified from a TILLING library (Taniguchi et al., 2006) and characterized as described in the Supplemental Experimental Procedures; the *foxn1:mCherry* transgenic zebrafish line has been described previously (Hess and Boehm, 2012).

Immunological and Histological Procedures

Phenotyping and preparative isolation of cell populations was performed by flow cytometry; the antibody response of mice was examined by immunization with nitrophenol coupled to chicken γ-globulin. For T cell proliferation assays, lymph node cells were stimulated with soluble CD3ε antibody and the dilution of carboxyfluorescein succinimidyl ester (CSFE) determined by flow cytometry after 3 days of culture. Cell proliferation was determined by intraperitoneal injection of bromodeoxyuridine (BrdU) and analysis 4 hr later with anti-BrdU. Tissues for hematoxylin/eosin staining were fixed in modified Davidson's fluid (for details, see the Supplemental Experimental Procedures).

Molecular Biology Assays

Diversity of medaka TCR beta chains was determined by cloning and sequencing of *tcrb* genes from intestine; quantitative RT-PCR was carried out with a 7500 Fast Real-Time PCR System (Applied Biosystems). RNA In situ hybridization and X-gal staining were performed on sections or on whole mounts (for details, see the Supplemental Experimental Procedures).

Phylogenetic Analyses

The source sequences used for phylogenetic analyses are given in the Supplemental Experimental Procedures.

SUPPLEMENTAL INFORMATION

Supplemental Information includes Supplemental Experimental Procedures, six figures, and three tables and can be found with this article online at http://dx.doi.org/10.1016/j.celrep.2014.07.017.

AUTHOR CONTRIBUTIONS

J.B.S. and T.B. conceived and designed the study. J.B.S., D.N., C.C.B., C.H., A.H.-A., and T.B. created and characterized mouse mutants. A.T. and Y.T. identified fish *foxn1* mutants. A.W., N.N., I.H., and M.S. characterized fish lines. J.B.S. and T.B. wrote the paper. All authors contributed to the writing of the manuscript.

ACKNOWLEDGMENTS

We thank all members of the T.B. laboratory for discussions and help during various stages of this project, Dr. B. Kanzler for help with the generation of transgenic mice, Dr. S. Takeda for support during the identification of *O. latipes* mutants, A. Würch and S. Hobitz for help with cell sorting, and the Max Planck Society for financial support. J.B.S. was supported by an Overseas Biomedical Research Fellowship from the Australian National Health and Medical Research Council.

Received: February 24, 2014
Revised: May 22, 2014
Accepted: July 14, 2014
Published: August 14, 2014

REFERENCES

Akashi, K., Richie, L.I., Miyamoto, T., Carr, W.H., and Weissman, I.L. (2000). B lymphopoiesis in the thymus. J. Immunol. *164*, 5221–5226.

Anderson, G., and Jenkinson, E.J. (2001). Lymphostromal interactions in thymic development and function. Nat. Rev. Immunol. *1*, 31–40.

Awong, G., and Zuniga-Pflucker, J.C. (2011). Thymus-bound: the many features of T cell progenitors. Front. Biosci. (Schol. Ed.) *3*, 961–969.

Bajoghli, B., Aghaallaei, N., Hess, I., Rode, I., Netuschil, N., Tay, B.-H., Venkatesh, B., Yu, J.-K., Kaltenbach, S.L., Holland, N.D., et al. (2009). Evolution of genetic networks underlying the emergence of thymopoiesis in vertebrates. Cell *138*, 186–197.

Bajoghli, B., Guo, P., Aghaallaei, N., Hirano, M., Strohmeier, C., McCurley, N., Bockman, D.E., Schorpp, M., Cooper, M.D., and Boehm, T. (2011). A thymus candidate in lampreys. Nature *470*, 90–94.

Bleul, C.C., and Boehm, T. (2005). BMP signaling is required for normal thymus development. J. Immunol. *175*, 5213–5221.

Bleul, C.C., Corbeaux, T., Reuter, A., Fisch, P., Mönting, J.S., and Boehm, T. (2006). Formation of a functional thymus initiated by a postnatal epithelial progenitor cell. Nature *441*, 992–996.

Boehm, T. (2011). Design principles of adaptive immune systems. Nat. Rev. Immunol. *11*, 307–317.

Boehm, T., Hess, I., and Swann, J.B. (2012). Evolution of lymphoid tissues. Trends Immunol. *33*, 315–321.

Calderón, L., and Boehm, T. (2011). Three chemokine receptors cooperatively regulate homing of hematopoietic progenitors to the embryonic mouse thymus. Proc. Natl. Acad. Sci. USA *108*, 7517–7522.

Calderón, L., and Boehm, T. (2012). Synergistic, context-dependent, and hierarchical functions of epithelial components in thymic microenvironments. Cell *149*, 159–172.

Ceredig, R. (2002). The ontogeny of B cells in the thymus of normal, CD3 ε knockout (KO), RAG-2 KO and IL-7 transgenic mice. Int. Immunol. *14*, 87–99.

Chi, N.C., Shaw, R.M., De Val, S., Kang, G., Jan, L.Y., Black, B.L., and Stainier, D.Y.R. (2008). Foxn4 directly regulates *tbx2b* expression and atrioventricular canal formation. Genes Dev. *22*, 734–739.

Danilova, N., Visel, A., Willett, C.E., and Steiner, L.A. (2004). Expression of the winged helix/forkhead gene, *foxn4*, during zebrafish development. Brain Res. Dev. Brain Res. *153*, 115–119.

DeLuca, D., Wilson, M., and Warr, G.W. (1983). Lymphocyte heterogeneity in the trout, *Salmo gairdneri*, defined with monoclonal antibodies to IgM. Eur. J. Immunol. *13*, 546–551.

Feyerabend, T.B., Terszowski, G., Tietz, A., Blum, C., Luche, H., Gossler, A., Gale, N.W., Radtke, F., Fehling, H.J., and Rodewald, H.R. (2009). Deletion of Notch1 converts pro-T cells to dendritic cells and promotes thymic B cells by cell-extrinsic and cell-intrinsic mechanisms. Immunity *30*, 67–79.

Flores, K.G., Li, J., and Hale, L.P. (2001). B cells in epithelial and perivascular compartments of human adult thymus. Hum. Pathol. *32*, 926–934.

Frank, J., Pignata, C., Panteleyev, A.A., Prowse, D.M., Baden, H., Weiner, L., Gaetaniello, L., Ahmad, W., Pozzi, N., Cserhalmi-Friedman, P.B., et al. (1999). Exposing the human nude phenotype. Nature *398*, 473–474.

Hardy, R.R., and Hayakawa, K. (2001). B cell development pathways. Annu. Rev. Immunol. *19*, 595–621.

Hartenstein, V. (2006). Blood cells and blood cell development in the animal kingdom. Annu. Rev. Cell Dev. Biol. *22*, 677–712.

Hess, I., and Boehm, T. (2012). Intravital imaging of thymopoiesis reveals dynamic lympho-epithelial interactions. Immunity *36*, 298–309.

Hirano, M., Guo, P., McCurley, N., Schorpp, M., Das, S., Boehm, T., and Cooper, M.D. (2013). Evolutionary implications of a third lymphocyte lineage in lampreys. Nature *501*, 435–438.

Hozumi, K., Mailhos, C., Negishi, N., Hirano, K., Yahata, T., Ando, K., Zuklys, S., Holländer, G.A., Shima, D.T., and Habu, S. (2008). Delta-like 4 is indispensable in thymic environment specific for T cell development. J. Exp. Med. *205*, 2507–2513.

Kenins, L., Gill, J.W., Boyd, R.L., Holländer, G.A., and Wodnar-Filipowicz, A. (2008). Intrathymic expression of Flt3 ligand enhances thymic recovery after irradiation. J. Exp. Med. *205*, 523–531.

Koch, U., Fiorini, E., Benedito, R., Besseyrias, V., Schuster-Gossler, K., Pierres, M., Manley, N.R., Duarte, A., Macdonald, H.R., and Radtke, F. (2008). Delta-like 4 is the essential, nonredundant ligand for Notch1 during thymic T cell lineage commitment. J. Exp. Med. *205*, 2515–2523.

Kyewski, B., and Derbinski, J. (2004). Self-representation in the thymus: an extended view. Nat. Rev. Immunol. *4*, 688–698.

Li, S., Mo, Z., Yang, X., Price, S.M., Shen, M.M., and Xiang, M. (2004). *Foxn4* controls the genesis of amacrine and horizontal cells by retinal progenitors. Neuron *43*, 795–807.

Mathis, D., and Benoist, C. (2009). Aire. Annu. Rev. Immunol. *27*, 287–312.

Meier, N., Dear, T.N., and Boehm, T. (1999). *Whn* and *mHa3* are components of the genetic hierarchy controlling hair follicle differentiation. Mech. Dev. *89*, 215–221.

Miller, J.F. (1961). Immunological function of the thymus. Lancet *2*, 748–749.

Miyadai, T., Ootani, M., Tahara, D., Aoki, M., and Saitoh, K. (2004). Monoclonal antibodies recognising serum immunoglobulins and surface immunoglobulin-positive cells of puffer fish, torafugu (*Takifugu rubripes*). Fish Shellfish Immunol. *17*, 211–222.

Nakagawa, S., Gisselbrecht, S.S., Rogers, J.M., Hartl, D.L., and Bulyk, M.L. (2013). DNA-binding specificity changes in the evolution of forkhead transcription factors. Proc. Natl. Acad. Sci. USA *110*, 12349–12354.

Nehls, M., Pfeifer, D., Schorpp, M., Hedrich, H., and Boehm, T. (1994). New member of the winged-helix protein family disrupted in mouse and rat nude mutations. Nature *372*, 103–107.

Nehls, M., Kyewski, B., Messerle, M., Waldschütz, R., Schüddekopf, K., Smith, A.J., and Boehm, T. (1996). Two genetically separable steps in the differentiation of thymic epithelium. Science *272*, 886–889.

Peter, I.S., and Davidson, E.H. (2011). Evolution of gene regulatory networks controlling body plan development. Cell *144*, 970–985.

Petrie, H.T., and Zúñiga-Pflücker, J.C. (2007). Zoned out: functional mapping of stromal signaling microenvironments in the thymus. Annu. Rev. Immunol. *25*, 649–679.

Rodewald, H.-R. (2008). Thymus organogenesis. Annu. Rev. Immunol. *26*, 355–388.

Schlake, T., Schorpp, M., Nehls, M., and Boehm, T. (1997). The *nude* gene encodes a sequence-specific DNA binding protein with homologs in organisms that lack an anticipatory immune system. Proc. Natl. Acad. Sci. USA *94*, 3842–3847.

Sitnicka, E., Brakebusch, C., Martensson, I.-L., Svensson, M., Agace, W.W., Sigvardsson, M., Buza-Vidas, N., Bryder, D., Cilio, C.M., Ahlenius, H., et al. (2003). Complementary signaling through flt3 and interleukin-7 receptor α is indispensable for fetal and adult B cell genesis. J. Exp. Med. *198*, 1495–1506.

Sood, N., Chaudhary, D.K., Rathore, G., Singh, A., and Lakra, W.S. (2011). Monoclonal antibodies to snakehead, *Channa striata* immunoglobulins: detection and quantification of immunoglobulin-positive cells in blood and lymphoid organs. Fish Shellfish Immunol. *30*, 569–575.

Sood, N., Chaudhary, D.K., Singh, A., and Rathore, G. (2012). Monoclonal antibody to serum immunoglobulins of *Clarias batrachus* and its application in immunoassays. Gene *511*, 411–419.

Soskine, M., and Tawfik, D.S. (2010). Mutational effects and the evolution of new protein functions. Nat. Rev. Genet. *11*, 572–582.

Taniguchi, Y., Takeda, S., Furutani-Seiki, M., Kamei, Y., Todo, T., Sasado, T., Deguchi, T., Kondoh, H., Mudde, J., Yamazoe, M., et al. (2006). Generation of medaka gene knockout models by target-selected mutagenesis. Genome Biol. *7*, R116.

Vigliano, F.A., Losada, A.P., Castello, M., Bermúdez, R., and Quiroga, M.I. (2011). Morphological and immunohistochemical characterisation of the thymus in juvenile turbot (*Psetta maxima*, L.). Cell Tissue Res. *346*, 407–416.

Wilkins, A.S. (1997). Canalization: a molecular genetic perspective. BioEssays *19*, 257–262.

Wilson, A., MacDonald, H.R., and Radtke, F. (2001). Notch 1-deficient common lymphoid precursors adopt a B cell fate in the thymus. J. Exp. Med. *194*, 1003–1012.

Zachariah, M.A., and Cyster, J.G. (2010). Neural crest-derived pericytes promote egress of mature thymocytes at the corticomedullary junction. Science *328*, 1129–1135.

Zamisch, M., Moore-Scott, B., Su, D.M., Lucas, P.J., Manley, N., and Richie, E.R. (2005). Ontogeny and regulation of IL-7-expressing thymic epithelial cells. J. Immunol. *174*, 60–67.